

## NUMERICAL STUDY ON UNCERTAINTY EFFECTS IN INJECTION MOLDING

F. Wittemann<sup>1\*</sup>, L. Kärger<sup>1</sup>

<sup>1</sup> Institute of Vehicle System Technology (FAST), Karlsruhe Institute of Technology (KIT),  
Karlsruhe, Germany,

\* Corresponding author (florian.wittemann@kit.edu)

**Keywords:** Injection molding simulation, process uncertainty, parameter variation, fiber reinforced polymers

### ABSTRACT

Injection molding is one of the most widely used processes to manufacture polymer parts, but due to uncertainties in material and process, the part quality scatters, which leads to a raising of safety factors and therefore to inefficient material use. Although current simulation approaches predict the manufacturing process and resulting part behavior quite well, the approaches are deterministic, and the simulated material is based on average data in most cases. This work presents an approach for fast approximation of cavity pressure under the consideration of uncertainties in material state and process temperatures. The approach is based on interpolation and superposition of a few process simulations and enables fast data creation for uncertainty studies. The results are in good agreement with deterministic simulations and experimental data.

### 1 INTRODUCTION

Nowadays, injection molding is one of the most important processes for mass production of polymer parts in various application fields. Especially, if fiber reinforced polymers (FRPs) are used, but also for pure polymer production, the manufacturing underlies uncertainties, caused by material (i.e. curing, aging, fiber distribution, contamination, etc.) and process (i.e. heating and cooling, friction, etc.). These phenomena lead to uncertainties in the manufacturing process, which is for example visible in the cavity pressure, and to uncertainties in the part quality, resulting in scattering of mechanical properties [1]. Jansen et al. [2] and Kurt et al. [3] investigate the influence of process conditions on shrinkage in thermoplastic injection molding, both name material temperature as important aspect. Mesogitis et al. [4] name the material state (storage, pre-curing, contaminations, humidity, etc.) as important aspect for process uncertainty and degradation of part properties for mold filling with thermoset matrix materials. This also applies for thermoset injection molding with discontinuous fibers, where uncertainties in material and process conditions influence the flow field and therefore the resulting fiber orientation, being crucial for the thermo-mechanical properties of the part. These uncertainties raise the safety factors, when using FRP parts, which lowers the effective use of material and has a negative impact on lightweight potential, CO<sub>2</sub>-footprint and costs.

Today's simulation approaches for injection molding are good in prognosing material flow and hence aspects like in-mold pressure, fiber orientation and phase changes [5–8]. These aspects are important to verify the manufacturability and are an important input for ongoing structural and warpage analysis [9,10]. However, these simulation approaches are deterministic and the representation of uncertainties in material and process come along with high numerical effort, by performing different single deterministic simulations.

This work presents numerical studies for injection molding trials, where the tool temperature, initial material temperature, initial curing state and fiber length are varied to show the individual influence on in-mold pressure. The simulations are compared to experimental results. An interpolation scheme offers the possibility for fast pressure prediction, when varying these parameters. The scheme can be used to approximate the scatter of in-mold pressure with respect to material and process uncertainties by performing only a few process simulations.

## 2 SIMULATION MODEL AND PARAMETER VARIATION

### 2.1 Injection molding simulation approach

To simulate the injection molding process, the methods presented in our previous work [5,6] are used. The previous work [6] presents a simulation approach, representing the material's viscosity with a fourth-order viscosity tensor, considering matrix viscosity, fiber orientation, volume fraction, and length. Hence, the fiber re-orientation and the variation of fiber length are captured by the flow modeling, influencing the predicted in-mold pressure, being an important aspect for process uncertainties, caused by fiber length variations. The matrix viscosity is modeled temperature, shear-rate and curing dependent with the approach presented by Castro and Macosko [11]. The curing kinetics are modeled with the Kamal-Malkin approach [12]. The fiber orientation is represented by a second-order orientation tensor, according to the work of Advani and Tucker [13] and modeled with the RSC-model, presented by Wang et al. [14]. For closure approximations, the IBOF5 approach is used [15]. This combination of modeling approaches was experimentally validated as suitable for injection molding simulation of discontinuous short fiber reinforced thermoset materials [6,16].

### 2.1 Experimental setup and parameter variation

The experimental setup and simulated cavity is a rectangular plate with  $480 \text{ mm} \times 190 \text{ mm} \times 2 \text{ mm}$ . The material enters the plate via a  $185 \text{ mm}$  long cone sprue at the plate's center, with a start diameter of  $9 \text{ mm}$  (Nozzle) and an end diameter of  $15.5 \text{ mm}$  (Sprue transfer). The cavity contains two pressure sensors at the  $x_2$ -plane of symmetry, with a distance of  $P_1 = 65 \text{ mm}$  and  $P_2 = 145 \text{ mm}$  from the center, as shown in Figure 1. The used material is a  $37.5 \text{ weight-}\%$  glass fiber filled phenolic. The fibers are assumed to have a constant length of  $L_F = 0.38 \text{ mm}$  and the initial curing state is assumed to be  $c_0 = 10 \%$ . The material is injected with a temperature of  $T_{\text{Mat}} = 120 \text{ }^\circ\text{C}$  and the mold is heated to  $T_{\text{Tool}} = 175 \text{ }^\circ\text{C}$ , as given in Table 1.

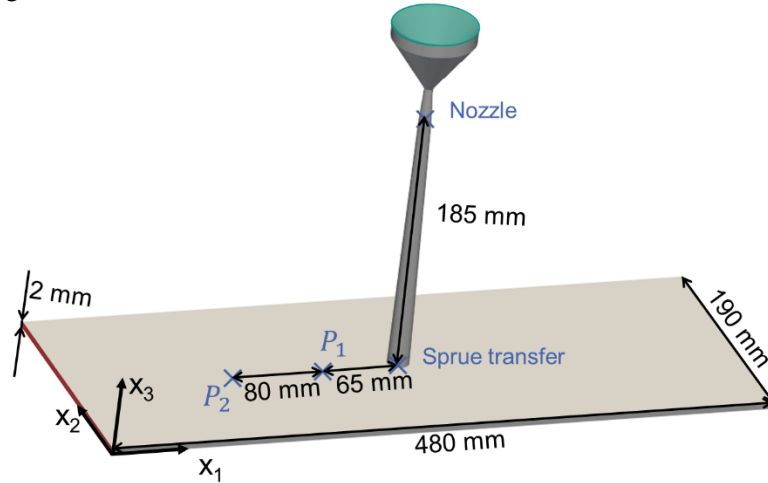


Figure 1: Cavity for experiments and simulation with position of pressure sensors. Inlet in green, outlet in red.

Parameter	$\pm 10 \%$ value	Mean value	$\pm 10 \%$ value
$T_{\text{Tool}}$	$157.5 \text{ }^\circ\text{C}$	$175 \text{ }^\circ\text{C}$	$192.5 \text{ }^\circ\text{C}$
$T_{\text{Mat}}$	$108 \text{ }^\circ\text{C}$	$120 \text{ }^\circ\text{C}$	$132 \text{ }^\circ\text{C}$
$L_F$	$0.342 \text{ mm}$	$0.38 \text{ mm}$	$0.418 \text{ mm}$
$c_0$	$9 \%$	$10 \%$	$11 \%$

Table 1: Varied parameters with corresponding minimal, mean and maximal values for process simulation.

To estimate the natural uncertainties in the process, certain material and process parameters are deliberately varied in the simulations. The varied parameters are the tool temperature  $T_{\text{Tool}}$ , the initial

material temperature  $T_{Mat}$ , the constant average fiber length  $L_F$  and the initial degree of cure  $c_0$ . All parameters are varied  $\pm 2.5\%$ ,  $\pm 5\%$ ,  $\pm 7.5\%$  and  $\pm 10\%$ . The mean and  $\pm 10\%$  values are given in Table 1.

### 3 RESULTS

#### 3.1 Experimental and simulation results

Figure 2 shows the experimental pressure at  $P_1$  and  $P_2$  (black solid lines). The pressure at  $P_1$  is the curve rising earlier and higher, since  $P_1$  is located nearer to the injection point. The experimental lines represent the mean of 8 experiments, the minimum and maximum pressure in the experiments is illustrated by the grey shading. The green lines are the simulated reference pressure at  $P_1$  and  $P_2$ , calculated by applying the process parameters (mean values in Table 1). The additional curves are the  $\pm 10\%$  variations of  $T_{tool}$  (red, dashed),  $T_{Mat}$  (orange, dotted),  $L_F$  (dark blue, dashed-dotted) and  $c_0$  (light blue, dotted).

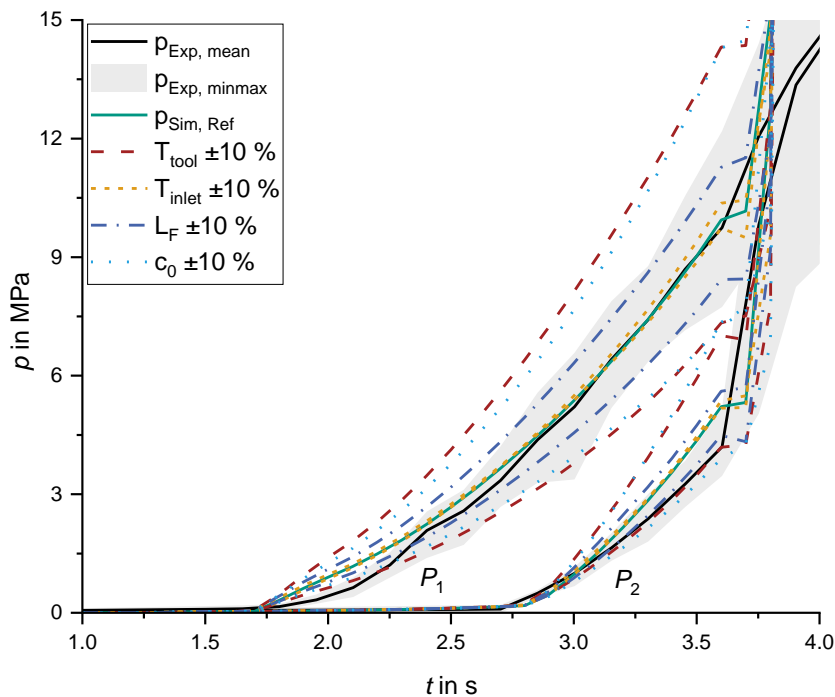


Figure 2: Pressure during filling at  $P_1$  and  $P_2$  in experiment (black), with scatter (grey). Corresponding simulation (green) with parameter variation  $\pm 10\%$  for  $T_{Tool}$  (red, dashed),  $T_{Mat}$  (orange, dotted),  $L_F$  (dark blue, dashed-dotted) and  $c_0$  (light blue, dotted).

The simulated reference pressure fits well at position  $P_1$  but is slightly too high at  $P_2$ , although the results are within the process uncertainty. The material's temperature at injection has nearly no influence on the predicted cavity pressure, as shown by the orange dotted lines. The small influence is due to the thin wall character of the geometry, with a constant thickness of 2 mm, making tool temperature dominant by the high surface-to-volume ratio. Therefore, the tool temperature shows the most significant influence of the four varied parameters on the simulated cavity pressure. At the end of fill (3.6 s) at  $P_1$  the pressure is about 44.5 % higher if  $T_{tool}$  is 10 % lower and about 26 % lower if  $T_{tool}$  is 10 % higher, compared to the reference simulation. One reason for this unsymmetric influence is the curing reaction. Raising the tool temperature lowers the viscosity and hence the pressure, but at the same time boosts the curing reaction, which rises the viscosity and hence the predicted pressure. The effect of lowering the tool temperature is vice versa. Since these effects are non-linear in the viscosity and the influence of curing and temperature is not equal, the influence is unsymmetric. The influence of the initial curing state is in the same range as the influence of the tool temperature, rising the simulated pressure about 44.4 % when rising  $c_0$  about 10 % and lowering the pressure about 26.6 % for lowering  $c_0$  about

10 %, compared to the reference simulation, at the end of fill and position  $P_1$ . The deviations due to  $T_{\text{tool}}$  and  $c_0$  for  $\pm 10$  % are greater than the experimental process uncertainty. The influence of fiber length is in a mean range, rising the pressure by about 13.8 %, when rising the fiber length by 10 %, and lowering the pressure by about 14.9 %, when lowering the fiber length by 10 %.

### 3.2 Results evaluation and deduction of systematics

As illustrated in Figure 2, the deviations in the simulations rise with the absolute value of the pressure, but the relative deviation is quite constant and similar at  $P_1$  and  $P_2$ . Hence, the relative offset of the cavity pressure should be approximable by knowing a reference pressure over time and constant parameter-specific influence factors. To verify this, the relative pressure deviation is evaluated for every parameter variation at different positions, being the nozzle, the transfer from the sprue to the plate, and the two sensor positions  $P_1$  and  $P_2$  (cf. Figure 1).

The results are shown in Figure 3 and the deviation  $\Delta p_{\text{rel}}$  due to the single parameters  $T_{\text{Mat}}$ ,  $L_F$  and  $c_0$  are similar at the different positions along the flow path. For  $T_{\text{tool}}$  the pressure change becomes smaller with greater distance from inlet, so the course of  $\Delta p_{\text{rel}}$  is flatter for  $P_2$ , compared to the nozzle. However,  $\Delta p_{\text{rel}}$  is still quite similar for  $T_{\text{tool}}$  at the different positions. The deviation is referred to a filling time of 3.5 s, so the material has reached every considered point in the cavity. The deviations do not only seem to be independent of the position in the cavity, the relative pressure deviation and percentual variation of parameters offer a linear relationship, as indicated by the linear regression lines in Figure 3. Hence, the relative pressure deviation  $\Delta p_{\text{rel}}$  can be approximated by a linear function

$$\Delta p_{\text{rel}} = a \cdot \Delta \lambda_{\text{rel}} + b \quad (1)$$

depending on the relative parameter variation  $\Delta \lambda_{\text{rel}}$ .

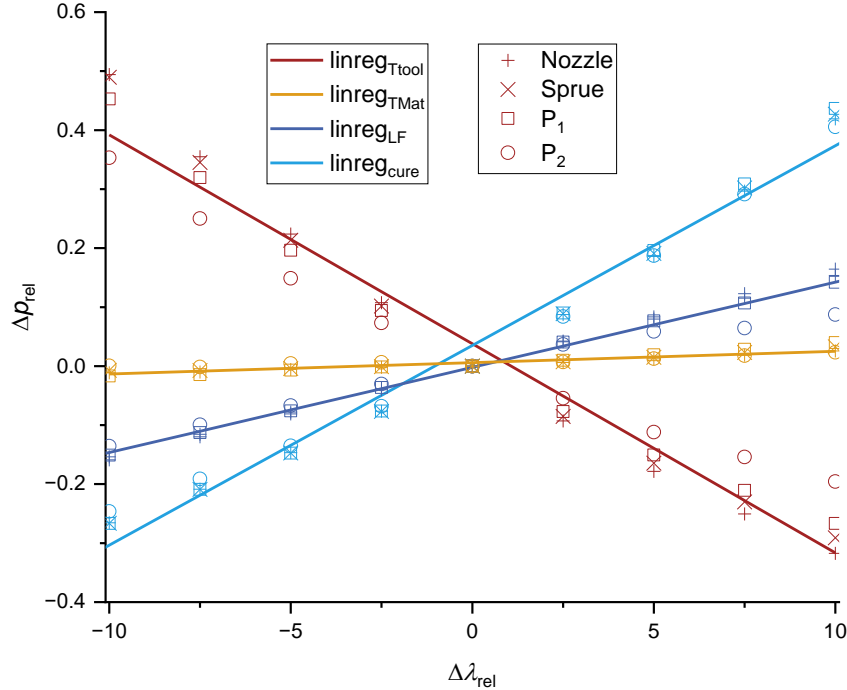


Figure 3 Relative pressure deviations for variation of  $T_{\text{Tool}}$  (red),  $T_{\text{Mat}}$  (orange),  $L_F$  (dark blue) and  $c_0$  (light blue), each at four different positions nozzle (+), sprue (x),  $P_1$ (square) and  $P_2$  (circle) along the flow path (cf. Figure 1), with corresponding linear regression lines.

The values of the determination coefficient  $R^2$ , representing the quality of the regression are given in Table 2. Besides  $T_{\text{Mat}}$  with  $R^2=0.84$ , all other  $R^2$  are  $>0.95$ , highlighting that  $\Delta p_{\text{rel}}$  can be well approximated by a linear function. The value for  $T_{\text{Mat}}$  is still in acceptable agreement, however, the influence of  $T_{\text{Mat}}$  on cavity pressure is small, as shown in Figure 2 and Figure 3. Therefore, the relative

deviation of pressure is describable by a simple linear function. The pressure variation caused by parameter variation can thus be determined by this linear function and a corresponding reference pressure, which is discussed in the next section.

Parameter	$R^2$
$T_{\text{Tool}}$	0.96
$T_{\text{Mat}}$	0.84
$L_{\text{F}}$	0.98
$c_0$	0.98

Table 2: Coefficient of determination for linear approximation of  $\Delta p_{\text{rel}}$  for different parameters.

#### 4 APPROXIMATION OF CAVITY PRESSURE FOR VARYING PARAMETERS

The resulting pressure due to parameter variation is approximated by means of the individual absolute pressure changes

$$\Delta p_{\text{abs}}(x_i, t) = \Delta p_{\text{rel}} \cdot p_{\text{Sim,Ref}}(x_i, t), \quad (2)$$

where  $p_{\text{Sim,Ref}}(x_i, t)$  is the simulated reference pressure (Figure 2, green) depending on the position  $x_i$  and time  $t$  and  $\Delta p_{\text{rel}}$  are the relative pressure changes (Eq. 1) for the individual changes of  $T_{\text{Tool}}$ ,  $T_{\text{Mat}}$ ,  $L_{\text{F}}$  and  $c_0$ . The approximated pressure  $p_{\text{ApX}}$  is then given by the superposition of the individual pressure changes  $\Delta p_{\text{abs}}$ , so

$$p_{\text{ApX}}(x_i, t) = p_{\text{Sim,Ref}}(x_i, t) + \Delta p_{\text{abs}, T_{\text{Tool}}}(x_i, t) + \Delta p_{\text{abs}, T_{\text{Mat}}}(x_i, t) + \Delta p_{\text{abs}, L_{\text{F}}}(x_i, t) + \Delta p_{\text{abs}, c_0}(x_i, t) \quad (3)$$

This approach is chosen to approximate the pressure with the simplest possible mathematical approach and hence minimal numerical effort. Simplest possible in this case means, that every position within the mold is modeled with the same function and this function is linear. Therefore, if this procedure is performed again, two simulations, evaluated at one position would contain all needed input for the approximation.

The linear regression is not forced to contain  $[\Delta \lambda_{\text{rel}}, \Delta p_{\text{rel}}] = [0, 0]$  and therefore the reference case is not exactly rebuilt. This condition is chosen, so the linear approximation is able to predict unsymmetric values of  $\Delta p_{\text{rel}}$  for  $\pm \Delta \lambda_{\text{rel}}$ . Hence, the regression is able to predict the unsymmetric behavior obtained in Figure 2, being especially relevant for  $T_{\text{Tool}}$  and  $c_0$ . As a result, the chosen approach should create too high pressures for low deviations, near the reference case due to the positive  $\Delta p_{\text{abs}, T_{\text{Tool}}}$  and  $\Delta p_{\text{abs}, c_0}$  at  $\Delta \lambda_{\text{rel}}=0$ .

Eq. (3) can be used to quickly approximate the pressure for specific parameter variations, or to approximate process uncertainties for random parameter input. For that purpose, 100 approximations of the pressure at  $P_1$  and  $P_2$  are created with random variation of  $T_{\text{Tool}}$ ,  $T_{\text{Mat}}$ ,  $L_{\text{F}}$  and  $c_0$ . To determine the random variation,  $\Delta \lambda_{\text{rel}}$  is calculated with a normal probability density function, with a mean of 0 and variation of  $\sigma^2=5$  for every parameter individually.

To validate the pressure approximation, it is compared to full 3D process simulations, performed with identical input parameters. Three specific parameter configurations of the 100 randomly created cases are chosen to compare the approximation and simulation. The three cases are chosen to result in a lower, similar and higher pressure, compared to the experimental data. The results are shown in Figure 4 for the 3D-simulations (solid lines) and approximation (dashed lines), the deviations of  $T_{\text{Tool}}$ ,  $T_{\text{Mat}}$ ,  $L_{\text{F}}$  and  $c_0$  (input parameters) are given in Table 3. Additionally, Figure 4 contains two simulations with  $\Delta \lambda_{\text{rel}}=\pm 5$ , resulting in a high pressure (orange,  $\Delta \lambda_{\text{rel}}=-5$  for  $T_{\text{Tool}}$  and  $\Delta \lambda_{\text{rel}}=5$  for  $T_{\text{Mat}}$ ,  $L_{\text{F}}$  and  $c_0$ ) and low pressure (light blue,  $\Delta \lambda_{\text{rel}}=5$  for  $T_{\text{Tool}}$  and  $\Delta \lambda_{\text{rel}}=-5$  for  $T_{\text{Mat}}$ ,  $L_{\text{F}}$  and  $c_0$ ). These configurations are chosen to generate low and high pressure, but with parameter values used to determine the linear function for the approximation.

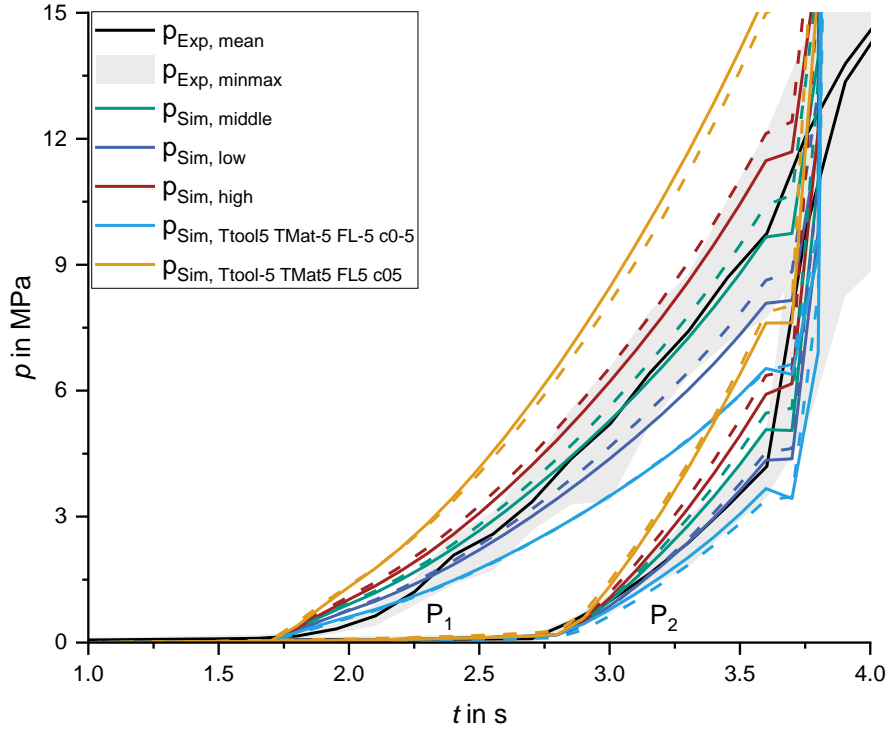


Figure 4: Pressure during filling at  $P_1$  and  $P_2$  in experiment (black), with scatter (grey). 3D-Simulation with random parameters with resulting low pressure (dark blue), middle pressure (green), high pressure (red), low pressure for  $\Delta\lambda_{\text{rel}} = \pm 5$  (light blue) and high pressure for  $\Delta\lambda_{\text{rel}} = \pm 5$  (orange). Corresponding approximations in dashed lines.

Due to the high degree of simplification and mentioned deviation of the approximation for low deviations of  $T_{\text{Tool}}$  and  $c_0$  the approximation calculates the pressure too high for configurations near the reference case, but within an acceptable range. The simulations with  $\Delta\lambda_{\text{rel}} = \pm 5$  are clearly out of the range of experimental data, so higher values of  $\Delta\lambda_{\text{rel}}$  would not be meaningful. For  $\Delta\lambda_{\text{rel}} = \pm 5$  simulation and approximation fit well. The average and maximum deviation between approximation and simulation are given in Table 4. The evaluation shown in Table 4 is only related to the time period of FRP flow at the positions, being 1.8 s to 3.7 s for  $P_1$  and 2.8 s to 3.7 s for  $P_2$ . The average deviation is less than 10 % at  $P_1$  and less than 15 % at  $P_2$  for every configuration, highlighting that the approximation is able to predict the cavity pressure adequately. The maximum deviation of 59 % at  $P_2$  in the simulation case  $p_{\text{Sim}, T_{\text{Tool}}=5 T_{\text{Mat}}=5 L_{\text{F}}=5 c_0=5}$  is high compared to the others, but appears directly at the beginning, so the absolute deviation is only about 0.15 MPa.

Parameter	$\Delta\lambda_{\text{rel}}$		
	$p_{\text{Sim}, \text{low}}$	$p_{\text{Sim}, \text{middle}}$	$p_{\text{Sim}, \text{high}}$
$T_{\text{Tool}}$	0.59	-1.2	-1.81
$T_{\text{Mat}}$	-2.87	1.59	0.71
$L_{\text{F}}$	-4.38	-0.44	-2.78
$c_0$	-3.36	-1.86	3.36

Table 3: Randomly determined parameter configurations for Simulations shown in Figure 4.

Although the approximation contains strong simplification to generate a simple and effective scheme, able to create data fast, the results are in an acceptable range. One reason for the deviation is of course the linear approximation itself, used to calculate  $\Delta p_{\text{rel}}$ . Another reason might be that the approximation

scheme determines the pressure change due to  $T_{Tool}$ ,  $T_{Mat}$ ,  $L_F$  and  $c_0$  completely independently, while there is an influence in the real process as well as in the 3D-simulations, for example the influence of shear heating or temperature on curing kinetics and viscosity.

The 100 approximations with randomly created input parameters are further used to create pressure curves for  $P_1$  and  $P_2$  with corresponding mean value and scatter to approximate the impact of manufacturing uncertainties on the in-mold pressure. The results are compared to the experimental data and shown in Figure 5.

Simulation case	Deviation of $p_{Apx}$ to $p_{Sim}$ in %			
	Average		Maximum	
	$P_1$	$P_2$	$P_1$	$P_2$
$p_{Sim,low}$	5.6	6.3	9.1	17.5
$p_{Sim,middle}$	5.9	6.9	12.1	17.4
$p_{Sim,high}$	6.3	11.1	11.9	21.6
$p_{Sim,T_{Tool}5 T_{Mat}5 L_F5 c_05}$	2.8	2.1	19.4	59
$p_{Sim,T_{Tool}5 T_{Mat}5 L_F5 c_05}$	4.3	10	17.2	28.8

Table 4: Average and maximum deviation of approximated pressure compared to simulated pressure for different parameter configurations.

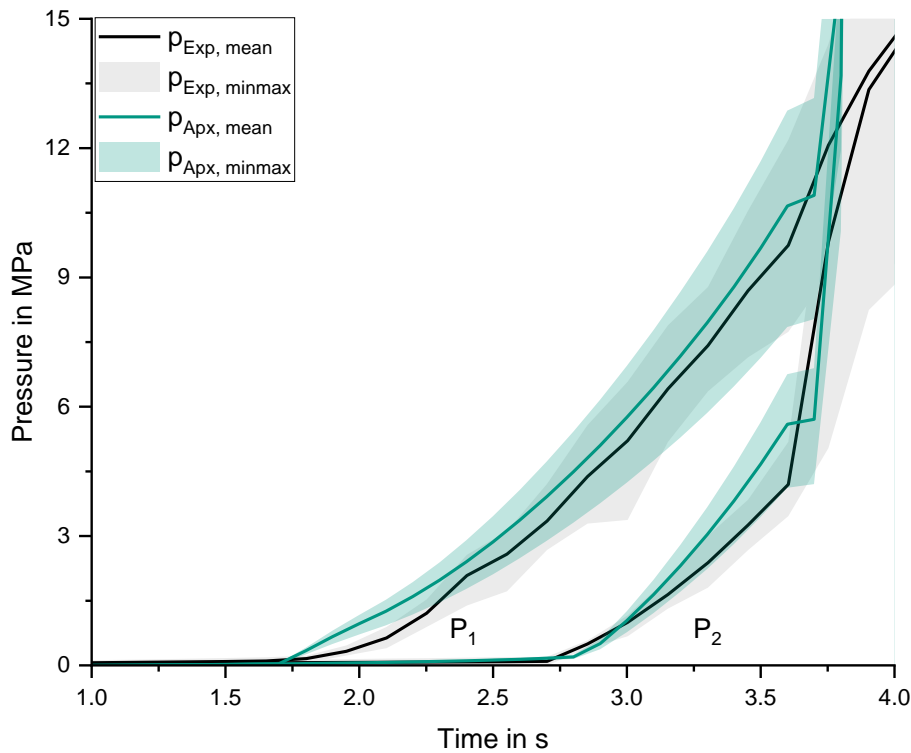


Figure 5: Pressure during filling at  $P_1$  and  $P_2$  in experiment (black), with scatter (grey). Mean curves of 100 approximated pressure curves (green) created with randomly chosen input parameters and corresponding scatter (light green).

As before, the averaged pressure prognosticated by the approximation is slightly too high but fits well at  $P_1$ , while it is too high and partially out of scatter at  $P_2$ . Similar, the scatter fits well at  $P_1$  and is slightly too high at  $P_2$ , compared to the scatter of experimental data. Therefore, the approximation scheme is able to estimate the manufacturing uncertainties of in-mold pressure with respect to the

parameters  $T_{\text{Tool}}$ ,  $T_{\text{Mat}}$ ,  $L_F$  and  $c_0$  in an efficient way, although in combination with strong simplifications. The scheme only needs a few 3D-simulation to create the data needed to approximate the pressure offset. The creation of the 100 pressure curves with random input took a few seconds on a normal computer, while one full 3D-simulation of this part takes a few hours on a 16-core workstation.

## 5 CONCLUSIONS

A novel scheme to efficiently approximate in-mold pressure in injection molding with manufacturing uncertainties is presented. The scheme represents one very simple linear approximation for the complete mold and therefore needs only a few 3D process simulations as input to approximate the pressure changes due to variation of initial mold and material temperature, as well as fiber length and initial curing state. The scheme represents a first step for efficient modeling of process uncertainties with a normal probability distribution function as input for parameter variation. More complex approximation function or position sensitive approaches may create better approximation results but come along with more effort to determine needed input. The aim was to evaluate the approximation results for one of the simplest approaches and the results are in good agreement to simulation data, related to the degree of simplification.

The scheme can also be used to determine the probability of a specific pressure profile due to process and material parameter uncertainty. This information may be a base to estimate part properties and make conclusions about the probability of the appearance of voids, unstable process routes, etc. due to uncertainties in material and process. Furthermore, it can be used to create data with little numerical effort, which then can be used to train neural networks.

Although the scheme is able to approximate pressure under uncertainties, it comes along with many simplifications and assumptions. Further research is needed to ascertain the potentials and limitations of the approach. Within this work, a simple rectangular plate is regarded, and it should be proofed, that the approximation also works for more complex geometries. At the moment, the scheme considers variation of input parameters, but they are still constant within one realization over time, while they also scatter over time in the real process. Another interesting aspect would be the approximation of further part properties like the final fiber orientation and curing state, being important input values for ongoing structural analysis. A fast and efficient prediction of these aspects would gain more knowledge about part behavior within manufacturing uncertainties and help to reduce risks and safety factors for injection molded parts.

## ACKNOWLEDGEMENTS

We would like to thank the ‘Deutsche Forschungsgemeinschaft’ (DFG) for funding the research project ‘MeproSi’ (project number: 464119659), which enabled this work.

## REFERENCES

- [1] English S. "Strukturbiildung bei der Verarbeitung von glasfasergefüllten Phenolformaldehydharzformmassen", doctoral thesis, Universitätsverlag Chemnitz, 2015.
- [2] K. M. B. Jansen, D. J. van Dijk, M. H. Husselman "Effect of processing conditions on shrinkage in injection molding". *Polym. Eng. Sci.*, **38**, 1998, pp 838–46.
- [3] M. Kurt, Y. Kaynak, O. S. Kamber, B. Mutlu, B. Bakir, U. Koklu "Influence of molding conditions on the shrinkage and roundness of injection molded parts". *Int J Adv Manuf Technol*, **46**, 2010, pp 571–8.
- [4] T. S. Mesogitis, A. A. Skordos, A. C. Long "Uncertainty in the manufacturing of fibrous thermosetting composites: A review". *Composites Part A: Applied Science and Manufacturing*, **57**, 2014, pp 67–75.
- [5] F. Wittemann, R. Maertens, A. Bernath, M. Hohberg, L. Kärger, F. Henning "Simulation of Reinforced Reactive Injection Molding with the Finite Volume Method". *J. Compos. Sci.*, **2**, 2018, pp 5.
- [6] F. Wittemann, R. Maertens, L. Kärger, F. Henning "Injection molding simulation of short fiber



- reinforced thermosets with anisotropic and non-Newtonian flow behavior". *Composites Part A: Applied Science and Manufacturing*, **124**, 2019, pp 105476.
- [7] J. Tamil, S. H. Ore, K. Y. Gan, S. H. Ore, K. Y. Gan, Y. Y. Bo, G. Ng, P. T. Wah, N. Suthiwongsunthorn, S. Chungpaiboonpatana "Molding Flow Modeling and Experimental Study on Void Control for Flip Chip Package Panel Molding with Molded Underfill Technology". *International Symposium on Microelectronics*, **2011**, 2012 // 2011, pp 673–82.
- [8] Ospald F. "Numerical Simulation of Injection Molding using OpenFOAM". *Proc. Appl. Math. Mech.*, **14**, 2014, pp 673–4.
- [9] J. Görthofer, N. Meyer, T. D. Pallicity, L. Schöttl, A. Trauth, M. Schemmann, M. Hohberg, P. Pinter, P. Elsner, F. Henning et al. "Virtual process chain of sheet molding compound: Development, validation and perspectives". *Composites Part B: Engineering*, **169**, 2019, pp 133–47.
- [10] L. Kärger, A. Bernath, F. Fritz, S. Galkin, D. Magagnato, A. Oeckerath, A. Schön, F. Henning "Development and validation of a CAE chain for unidirectional fibre reinforced composite components". *Composite Structures*, **132**, 2015, pp 350–8.
- [11] J. M. Castro, C. W. Macosko "Studies of mold filling and curing in the reaction injection molding process". *American Institute of Chemical Engineers Journals*, **28**, 1982, pp 250–60.
- [12] M. R. Kamal, S. Sourour "Kinetics and thermal characterization of thermoset cure". *Polym. Eng. Sci.*, **13**, 1973, pp 59–64.
- [13] S. G. Advani, C. L. Tucker "The Use of Tensors to Describe and Predict Fiber Orientation in Short Fiber Composites". *Journal of Rheology*, **31**, 1987, pp 751–84.
- [14] J. Wang, J. F. O'Gara, C. L. Tucker "An objective model for slow orientation kinetics in concentrated fiber suspensions: Theory and rheological evidence". *Journal of Rheology*, **52**, 2008, pp 1179–200.
- [15] H. Du Chung, T. H. Kwon "Invariant-based optimal fitting closure approximation for the numerical prediction of flow-induced fiber orientation". *Journal of Rheology*, **46**, 2002, pp 169–94.
- [16] F. Wittemann, L. Kärger, F. Henning "Influence of fiber breakage on flow behavior in fiber length- and orientation-dependent injection molding simulations". *Journal of Non-Newtonian Fluid Mechanics*, **310**, 2022, pp 104950.